Mechanisms of Chronic Skin Ulceration Linking Lactate, Transforming Growth Factor-β, Vascular Endothelial Growth Factor, Collagen Remodeling, Collagen Stability, and Defective Angiogenesis

Stephen John Dalton[1,2,3], Christine Vivienne Whiting[2,3], Jennifer Ruth Bailey[2], David Charles Mitchell[1] and John Francis Tarlton[2]

Up to one million people suffer from chronic skin ulcers in the US. Little is known of the mechanisms leading to tissue breakdown, although inadequate circulation and ischemia are common elements in most dermal ulcers. Collagen is the principal source of mechanical strength in most tissues, and its molecular and fibrillar stability is dependent on adequate oxygen supply. In wound repair, localized ischemia leads to fibrogenic responses culminating in elevated collagen synthesis and remodeling. This study examines factors influencing collagen turnover and stabilization before ulceration in "at risk" patients. Severely ischemic but uninjured ischemic skin (IS) was compared with patient- and site-matched non-ischemic skin. Biochemical mechanisms of tissue repair were activated in IS, with increased lactate, transforming growth factor-β, vascular endothelial growth factor, collagen synthesis and matrix metalloproteinases (MMPs)-1 and 2. The absence of MMP-9 and inflammatory cells confirmed that this upregulation was inappropriate and not in response to injury. Molecular stability of collagen was reduced in IS, and there was increased susceptibility to enzymic degradation. In conclusion, chronic ischemia and long-term hypoxia result in elevated collagen remodeling in an oxygen-poor environment. Unstable collagen molecules are synthesized together with upregulated MMPs, resulting in collagen denaturation, defective angiogenesis, weaker skin, and predisposition to ulceration.

Journal of Investigative Dermatology (2007) **127,** 958–968. doi:10.1038/sj.jid.5700651; published online 11 January 2007

INTRODUCTION

In the US up to one million people suffer from chronic leg ulcers, with profound effects on the quality of life, and a cost of $1.5–2 billion per annum (Harrington *et al.*, 2000). Ischemia secondary to peripheral vascular disease is a significant cause of ulceration, with a large proportion of leg ulcers of primarily venous or diabetic etiology also having an ischemic component (Cornwall *et al.*, 1986). Ulcers often arise following minimal trauma, and lead to significant morbidity, being the principal cause of lower limb amputation (London and Donnelly, 2000).

Studies investigating the pathology of chronic ulcers have concentrated on processes taking place after ulcers have formed (Tarlton *et al.*, 1999), with none having investigated processes that lead to the initial and progressive dermal failure in ulceration. Thus, the mechanisms of structural breakdown of the skin, and why ulcers form in the first place, are largely unknown (Nanney, 2005).

Lactate is generated in tissue hypoxia, and though largely a metabolite of skeletal muscle metabolism, skin is also a significant lactate source (Johnson and Fusaro, 1972). It has been measured *in vivo* by dermal microdialysis (Petersen, 1999); however, its direct measurement in skin biopsies and as a measure of dermal ischemia has not been reported. Lactate is an important mediator in the extracellular matrix. Addition to cultured fibroblasts significantly increases both their collagen (Klein *et al.*, 2001) and transforming growth factor-β (TGF-β) (Yalamanchi *et al.*, 2004) synthesis. Lactate also upregulates vascular endothelial growth factor (VEGF) synthesis (Constant *et al.*, 2000).

Collagen is the major component of the extracellular matrix, providing most of its mechanical strength and much of the organization of the scaffold on which cellular events

[1]*Department of Vascular Surgery, Southmead Hospital, Bristol, UK and* [2]*Matrix Biology Research Group, Veterinary Pathology, Infection and Immunity, School of Clinical Veterinary Science, University of Bristol, Bristol, UK*

[3]*These authors contributed equally to this work*

Correspondence: Dr John F. Tarlton, Matrix Biology Research Group, VPII, School of Clinical Veterinary Science, University of Bristol, Langford, BS40 5DU, UK. E-mail: john.tarlton@bristol.ac.uk

Abbreviations: IS, ischemic skin; MMP, matrix metalloproteinase; NI, non-ischemic; NIS, non-ischemic skin; PBS, phosphate-buffered saline; PICP, procollagen I C propeptide; TGFβ, transforming growth factor-β; TKR, total knee replacement; TR, TGFβ receptor; VV, varicose vein; VEGF, vascular endothelial growth factor

Received 12 May 2006; revised 13 September 2006; accepted 14 September 2006; published online 11 January 2007

occur. Type I collagen is the most abundant protein in skin. It is synthesized as three separate α chains that assemble within cells, such as fibroblasts, before secretion. Molecular oxygen is required for the enzymatic hydroxylation of proline and lysine, allowing stable triple helix formation before collagen fibril assembly (Kivirikko and Pihlajaniemi, 1998), and for lysyl oxidase-mediated crosslink formation during fibril stabilization (Miles *et al.*, 1995). Under-hydroxylation of the collagen molecule would influence its stability, susceptibility to enzymic degradation, mechanical strength of the skin, and the formation of new blood vessels. A parallel may be seen in scurvy (Akikusa *et al.*, 2003), in which reduced collagen hydroxylation owing to lack of ascorbate, a prolyl-4-hydroxylase cofactor, results in loss of strength in the skin, dysfunctional capillaries, and poor tissue repair.

TGF-*β* is integral in extracellular matrix remodeling (Stampfer *et al.*, 1993). It results in enhanced fibroblast migration (Mogford *et al.*, 2002) and proliferation (Strutz *et al.*, 2001), increases collagen (Bettinger *et al.*, 1996) and matrix metalloproteinase (MMP)-2 (Salo *et al.*, 1991) synthesis and has an angiogenic effect on endothelial cells (Berse *et al.*, 1999; Vinals and Pouyssegur, 2001). TGF-*β* signaling is mediated via two specific cell surface receptors, TRI and TRII. Constitutively active TRII permits dimer formation with TRI, its phosphorylation and signaling (Wrana *et al.*, 1994), with recruitment and phosphorylation of smad2 or smad3, which then dimerise with smad4 to initiate gene transcription. Smad6 and smad7, inhibit TGF-*β* signaling. Receptor binding can be enhanced via interaction with TGF-*β* RIII (betaglycan) or CD105 (endoglin) (Lopez-Casillas *et al.*, 1993; Sanchez-Elsner *et al.*, 2001). TRI and TRII are expressed on most cells, and TRIII and CD105 are highly expressed by endothelial cells (Wong *et al.*, 2000). CD105 is important in angiogenesis and is used as a marker of neovascularization (Duff *et al.*, 2003).

VEGF is a key angiogenic factor promoting endothelial cell proliferation, survival, and morphogenesis (Carmeliet, 2000). VEGF RII (KDR/Flk-1), expressed principally by endothelial cells, promotes proliferation, and is upregulated by VEGF (Shen *et al.*, 1998). VEGF RI (Flt-1), expressed by endothelial cells, fibroblasts, and leukocytes, is upregulated in hypoxia via hypoxia inducible factor-1α (Gerber *et al.*, 1997), and acts as a negative regulator of VEGF signaling probably by competing for ligand (Roberts *et al.*, 2004).

In acute wounds, disruption of the microvasculature leads to local hypoxia and elevated lactate. These factors stimulate collagen synthesis (Hunt *et al.*, 1978), with synergistic hypoxia inducible factor-1α and TGF-*β* signaling leading to elevated VEGF (Berse *et al.*, 1999; Sanchez-Elsner *et al.*, 2001) and CD105 (Sanchez-Elsner *et al.*, 2002) synthesis, and increased angiogenesis promoting tissue repair. Upregulated VEGF in human keratinocytes and dermal fibroblasts cultured in hypoxic conditions (Detmar *et al.*, 1997) has been shown to stimulate fibroblast TGF-*β* (Falanga *et al.*, 1991, 2002) and collagen synthesis (Falanga *et al.*, 2002).

Whether this mechanism also pertains secondary to generalized ischemia is not known. We have previously demonstrated that increased matrix remodeling occurs in non-injured ischemic skin (IS), which may predispose to dermal failure (Dalton *et al.*, 2005). However, the mechanistic link between matrix changes and chronic ischemia, and how this may lead to tissue breakdown, has not been established.

We hypothesize that inappropriate metabolic processes occurring in uninjured, chronically ischemic skin would result in elevated extracellular matrix turnover and defective matrix deposition, leading to mechanically weakened skin, and predisposition to the formation of ulcers.

RESULTS

Lactate

Tissue lactate levels were significantly elevated in IS samples (0.94 ± 0.09 mmol/l) (Figure 1a and b) when compared to the non-ischemic skin (NI) patient matched pairs (0.47 ± 0.07 mmol/l, $P < 0.001$). No difference was found in the lactate levels between NIS patient matched control and varicose vein (VV) (0.29 ± 0.02 mmol/l) and total knee replacement (TKR) (0.3 ± 0.05 mmol/l) controls (Figure 1a, $P > 0.05$ for both VV and TKR).

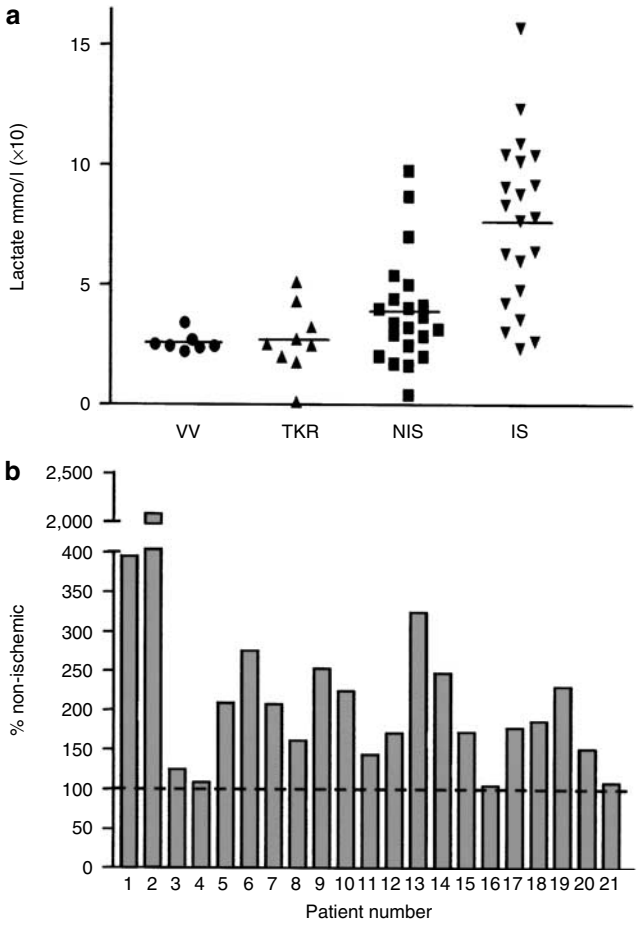

Figure 1. Lactate in IS and control skin measured by colorimetric assay. (**a**) Lactate levels in grouped ischemic samples compared to VV, TKR, and NI controls expressed in mmol/l ($P < 0.001$, unpaired *t*-test) and (**b**) lactate in individual ischemic samples expressed as a percentage of the matched NI values ($P < 0.001$, Wilcoxon's signed rank test).

TGF-β1

The level of TGF-β1 within tissue extract was significantly elevated in the IS (4.58±0.86 ng/ml) compared to matched paired NIS tissue (2.84±0.67 ng/ml) (Figure 2a and b, $P<0.05$); however, no significant correlation between lactate and TGF-β1 was demonstrated.

TGF-β receptor expression

TGF-β RI and II were expressed by keratinocytes, vessel endothelium and fibroblasts (Figure 3). TGF-β RI (Figures 3a, b and 4a) expression in the dermis (excluding large blood vessels) was significantly increased in IS ($P<0.01$). TRI expression was more prominent than TRII (Figure 3c and d) and cells expressing TRII (Figure 4b) occupied a smaller area of dermis (excluding large blood vessels) than TRI-expressing cells (Figure 4a), with no difference between the NIS and IS tissues; however, the distribution of cells expressing TRI and TRII was similar in both IS and NIS skin. Colocalization studies showed that TRI was predominantly expressed by fibroblasts ($5B5^+/TRI^+$) in the dermis with little expression by $CD45^+$ ($CD45^+/TRI^+$) immune cells (data not shown). Small vessels in the papillary dermis expressed both receptors at lower level than large vessels, with large vessel endothelium expressing both TRI and TRII at a level similar to that of keratinocytes (data not shown). TRIII was strongly expressed by keratinocytes and endothelium. There was no obvious increase in TRIII expression intensity by either celltype in IS, but there was an increase in vascularity in IS; therefore there was an increase in area tissue expression of TRIII (Figure 3e and f).

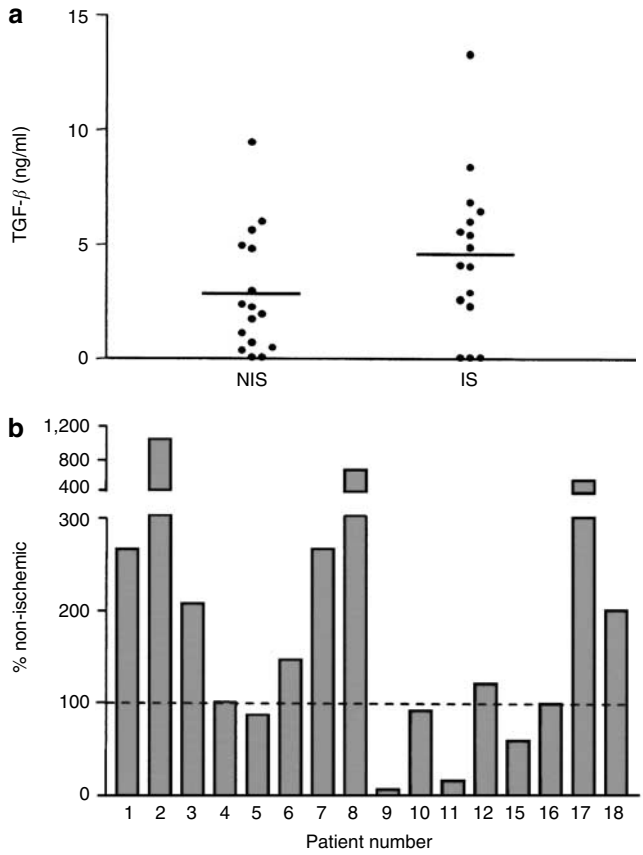

Figure 2. Level of TGFβ in IS and controls measured by ELISA. (**a**) Individual samples ($P<0.05$, Wilcoxon's signed rank test) and (**b**) ischemic samples expressed as a percent of NI-matched pairs ($P<0.05$, Wilcoxon's signed rank test).

Smad signaling

TGF-β signals predominantly via activation of smad2 and smad3, with subsequent negative regulation by smad7. The area of dermis expressing phosphorylated smad 2/3 was significantly increased ($P=0.031$) in IS (Figures 3g, h, and 4c), whereas areas of dermis expressing inhibitory smad7 were significantly decreased in IS skin ($P<0.014$) (Figures 3i, j and 4d). Large vessels (identified by morphology and serial sections stained with VEGFRII) expressed smad 2/3 and smad7 at a high level, and were excluded from analysis, but the expression of smad 2/3 and smad7 in the remaining dermis was relatively low; therefore small blood vessels, leukocytes, and fibroblasts were analyzed together. Preliminary data indicated that a similar pattern of expression was observed between an antibody against smad7 and that of an antibody detecting both smad6 and smad7 (data not shown). Immunoprecipitation of skin lysates for phosphorylated smad 2/3 revealed no difference between IS and NI skin (data not shown), most likely due to the high level of expression in keratinocytes and vessels in both groups (Figure 3h and j).

Collagen synthesis

Levels of type I collagen C propeptide (PICP), demonstrating increased collagen synthesis, were significantly increased in the IS (123.0±17.04 ng/mg) compared to NIS-matched paired samples (62.55±13.64 ng/mg) (Figure 5a and b, $P<0.001$), and also when compared to both the TKR (49.28±7.31 ng/mg) ($P<0.01$) and VV (46.64±8.07 ng/mg) ($P<0.005$) control tissues (Figure 5a). No significant difference was demonstrated between NIS patient matched control and VV or TKR controls (Figure 5a, $P>0.5$). A highly significant correlation was demonstrated between collagen synthesis and lactate levels (Figure 5c, $P<0.01$, and $r=0.42$).

VEGF

VEGF levels were highly elevated in IS (0.97±0.31 ng/mg) compared to NIS-matched paired samples (0.14±0.02 ng/mg) (Figure 6a and b, $P<0.01$). A close correlation was seen between lactate and VEGF levels (Figure 6c, $P<0.001$, $r=0.55$).

VEGF receptor expression

VEGR RI was expressed at low levels by endothelial cells, keratinocytes, and non-endothelial cells in the dermis in NIS (Figure 7a). A similar distribution and level of expression were observed in IS; there were, however, areas where elevated VEGF RI expression was associated with papillary vessels in IS (Figure 7b). VEGF RII expression was confined to vessel endothelium in the dermis of both NIS and IS samples

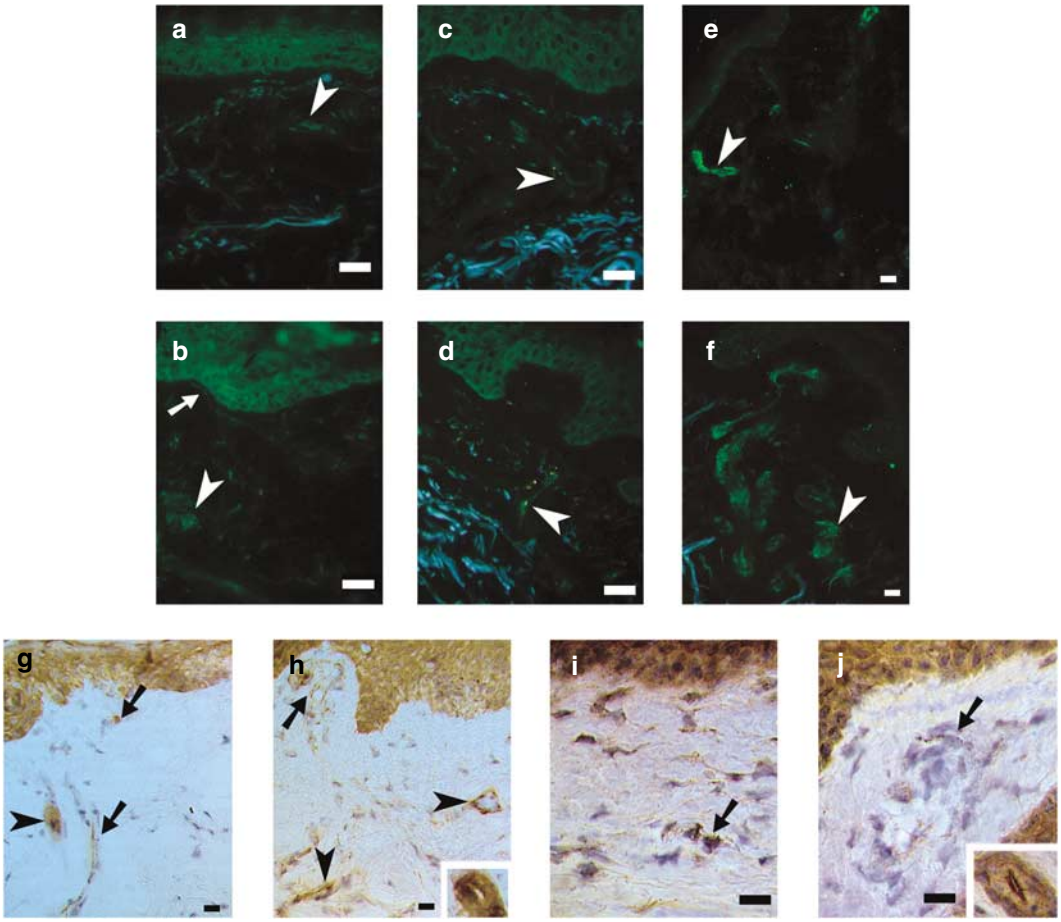

Figure 3. Immunohistological localization of TGF-β receptor I, II, and III, and TGF-β signaling intermediates, in IS and control skin. (**a**, **b**) TRI, (**c**, **d**) TRII, and (**e**, **f**) TRIII expression in (**a**, **c**, **e**) NI and (**b**, **d**, **f**) IS. (**a**, **b**) TRI expression was observed in keratinocytes, fibroblasts (small arrows), and vessel endothelium (arrowheads) in the papillary dermis. (**c**, **d**) TRII expression was expressed similarly to TRI, but at a much lower level by fibroblasts. (**e**, **f**) Keratinocytes and endothelium expressed TRIII. Phosphorylated (P) smad 2/3 expression in (**g**) NIS and (**h**) IS and smad7 expression in (**i**) NIS and (**j**) IS, arrows indicate small blood vessels and arrowheads indicate large vessels. Bar = 20 μm. Blue fibers in the dermis are due to autofluorescence.

(Figure 7c and d). Expression of VEGF RII was always associated with vascular endothelial basement membrane type IV collagen; however, both the area of endothelium expressing VEGF RII and the intensity of expression were elevated in IS (Figure 7d).

Angiogenesis

CD105 was strongly expressed by blood vessels and keratinocytes in both NIS and IS dermis (Figure 7e and f). Using CD105 as a marker for endothelium, which was clearly distinguishable morphologically from convoluted epidermis, it was observed that the area of CD105 in the dermis was significantly increased in IS ($0.06 \pm 0.01\ \mu m^2/\mu m^2$) compared to NIS ($0.028 \pm 0.005\ \mu m^2/\mu m^2$) ($P < 0.01$) (Figure 7g) and expression appeared elevated in IS samples (Figure 7i). In 12/16 IS samples, there were areas of vessel endothelium which expressed CD105 without colocalization with type IV collagen (Figure 7i), compared to only 1/16 NIS skin samples (Figure 7h). These areas of single CD105-positive endothelium were always close to the epidermis. An intact epidermal basement membrane was observed in both tissue groups.

Immune/inflammatory cells

CD45 is a pan immune cell marker labeling resident and infiltrating cells including lymphocytes, macrophages, and neutrophils. There was no significant difference in the area of dermis positive for CD45 between IS (7.1%) and NIS (5.6%, $P = 0.37$), demonstrating no inflammation in the IS samples.

Molecular stability

The temperature of denaturation of the collagen triple helix, T_{max}, in IS was significantly lower than NI-matched pairs (Figure 8a, $P = 0.02$).

Susceptibility to enzymic degradation

A significantly greater proportion of hydroxyproline was released by pepsin digestion in the ischemic samples compared with NI-matched pairs ($P = 0.01$, Figure 8b). Of

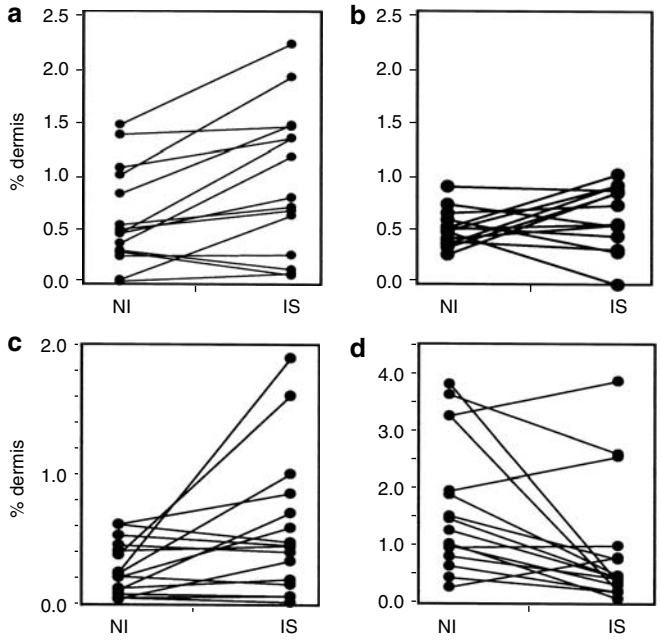

Figure 4. Image analysis of TGF-β receptor I, II, and TGF-β signaling molecules in IS and control skin. Area of dermis (excluding large blood vessels) expressing TRI and TRII. (**a**) TRI expression was significantly increased in IS, (**b**) whereas there was no change in TRII expression in IS. (**c**) Area of dermis expressing P-smad2/3 was increased in IS (large blood vessels excluded), (**d**) whereas smad7 expression was decreased in IS (large blood vessels excluded).

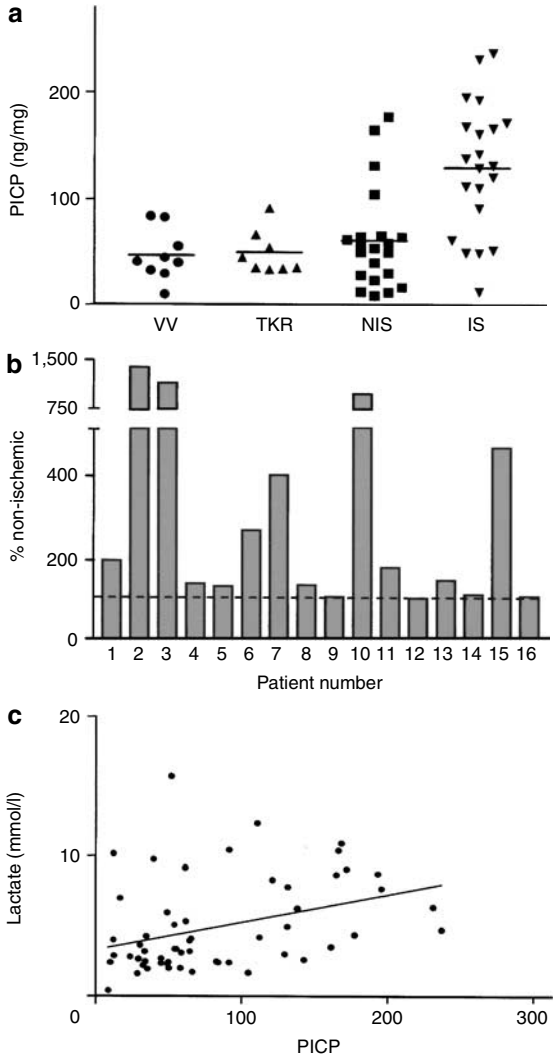

Figure 5. Type I collagen synthesis in IS and control skin measured by ELISA. (**a**) PICP levels in grouped ischemic samples compared to VV, TKR, and NI controls expressed as ng/mg ($P<0.001$, unpaired *t*-test) and (**b**) PICP in individual ischemic samples expressed as a percentage of the matched NI values ($P<0.001$, Wilcoxon's signed rank test). (**c**) Correlation between lactate and PICP levels ($P<0.01$ and $r=0.42$).

the 15 matched pairs, 12 demonstrated higher levels of collagen degraded in the ischemic samples.

Mechanical strength of ischemic and NIS

Owing to the nature of the material, difficulties were experienced fixing the skin in the Instron testing apparatus, including breakage at the clamp margins, slippage, and delamination. Despite these difficulties, IS was significantly weaker (reduced stress at failure) than NI-matched pairs (Figure 8c, $P<0.05$).

DISCUSSION

The pathophysiology of ulcer formation has received little attention, as studies have largely concentrated on processes taking place after ulcers have formed, such as impaired healing (Tarlton *et al.*, 1999). The factors which lead up to structural and functional failure of the skin are not known. Ischemia is a common element in ulcers of all etiologies, but how such ischemia contributes to ulcer formation in macroscopically normal skin is not known. We have previously reported that increased matrix remodeling occurs in IS (Dalton *et al.*, 2005). Here we reveal mechanisms linking tissue ischemia with the matrix changes that result in weakened skin, increased but defective angiogenesis, and a predisposition to ulcer formation.

Skin samples showed no physical evidence of injury, and baseline expression of MMP-9 (Dalton *et al.*, 2005), depressed smad7 expression and no increase in immune cells provided corroboration that the changes identified in IS occurred in the absence of injury or trauma.

Increased type I collagen synthesis was seen in all samples of uninjured IS, probably influenced by increased levels of lactate and TGF-β. Elevated lactate levels resulting from hypoxic metabolism have been demonstrated in porcine IS flaps (Mortazavi-Haghighat *et al.*, 2002), but this is the first report in ischemic human tissue. TGF-β increases collagen (Bettinger *et al.*, 1996) and MMP-2 (Salo *et al.*, 1991) synthesis, and lactate upregulates both collagen (Klein *et al.*, 2001) and TGF-β (Yalamanchi *et al.*, 2004) production *in vitro*. Falanga *et al.* (2002) demonstrated that hypoxia-stimulated collagen synthesis in cultured human fibroblasts, and that this was TGF-β1 dependent (Falanga *et al.*, 2002). Combined elevated collagen and MMP-2 synthesis

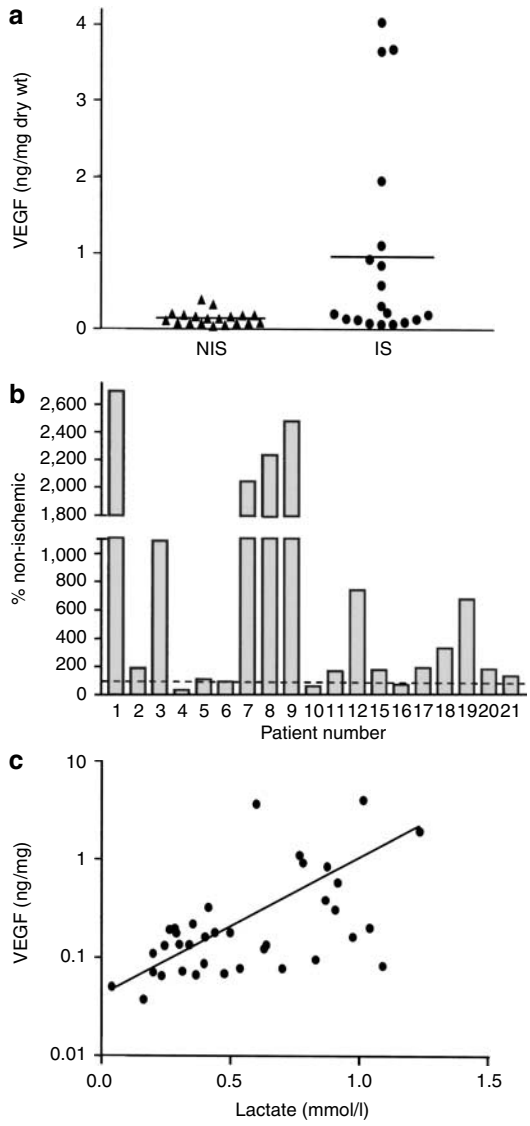

Figure 6. VEGF expression in IS and control skin measured by ELISA. VEGF levels in (**a**) grouped IS and control skin ($P<0.001$, Wilcoxon's signed rank test) and (**b**) individual ischemic samples expressed as a percentage of the matched NIS ($P<0.001$ Wilcoxon's signed rank test). (**c**) Correlation between VEGF and lactate (Pearson correlation, $P=0.0003$, $r^2=0.3048$).

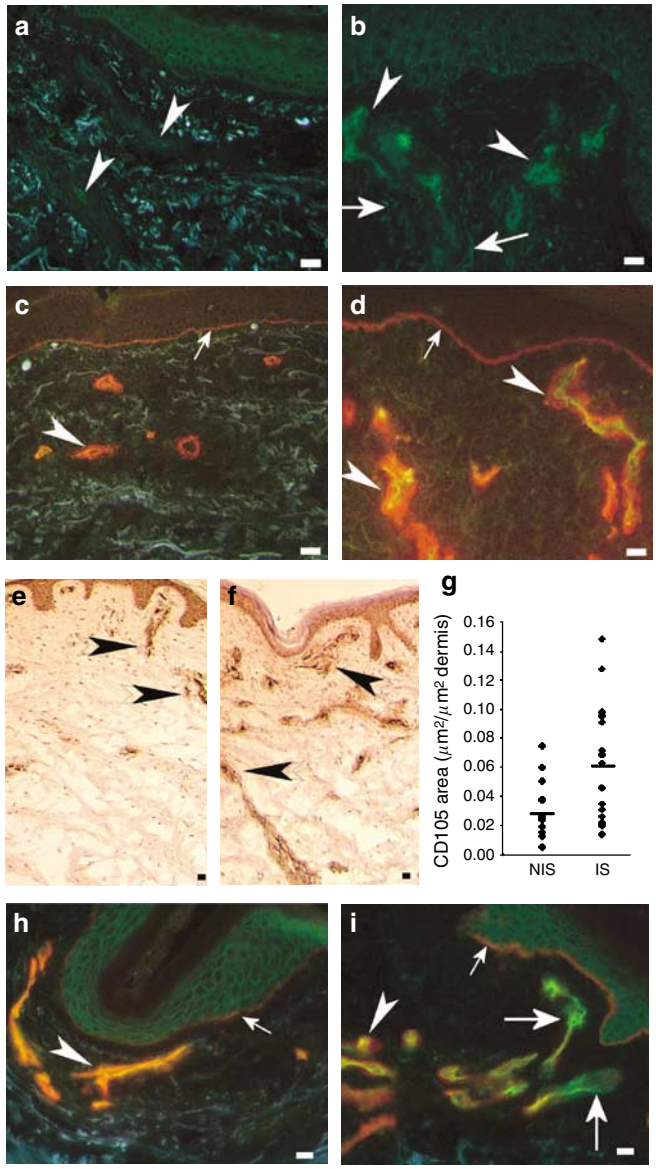

Figure 7. Immunohistological localization of CD105, VEGF receptors I and II, and Type IV collagen in IS and control skin. (**a**, **b**) VEGF RI, (**c**, **d**) VEGF RII, and (**e**–**i**) CD105 expression in (**a**, **c**, **e**, **h**) NI and (**b**, **d**, **f**, **i**) IS skin. (**a**, **b**) VEGF RI was expressed by vessel endothelium (large arrowheads) and non-endothelial cells (large arrows) in the dermis. (**c**, **d**) Endothelial VEGF RII (FITC) colocalized with basement membrane type IV collagen (Texas Red, overlapping expression with FITC is yellow, large arrowheads). (**e**, **f**) CD105 was expressed by vessel endothelium (arrow heads) and keratinocytes, and (**g**) the area of dermal expression significantly increased in IS ($P<0.01$). CD105 (FITC) colocalized with type IV collagen (Texas Red) in (**h**) NIS and (**i**) IS (large arrowheads), but in IS there were also areas where RII and type IV collagen were not coexpressed (large arrows). Epidermal basement membrane (small closed arrows, **c**, **d**, **h**, **i**). Bar = 20 μm. Blue fibers in the dermis are due to autofluorescence.

demonstrated increased matrix turnover which is inappropriate in uninjured skin (Dalton *et al.*, 2005).

Fibroblasts, which synthesize skin collagen, apparently expressed more TGF-βRI than TRII. Colocalization studies to determine which cell types within the dermis express TGF-βRI showed that TRI^+ cells were principally fibroblasts ($5B5^+$) rather than $CD45^+$ immune cells. The precise balance of receptor expression may result in differential effects, as RI mediates fibronectin synthesis, but growth inhibition is more dependent on TRII (Geiser *et al.*, 1992). TRI levels were significantly increased in ischemic dermis; therefore the increase in type I collagen synthesis in ischemic tissue was probably due to a combined effect of elevated TGF-β acting via increased dermal receptor expression by fibroblasts.

VEGF was also elevated in IS, which, like TGF-β, is a key factor promoting angiogenesis. TGF-β has been shown to promote endothelial cell survival and morphogenesis in

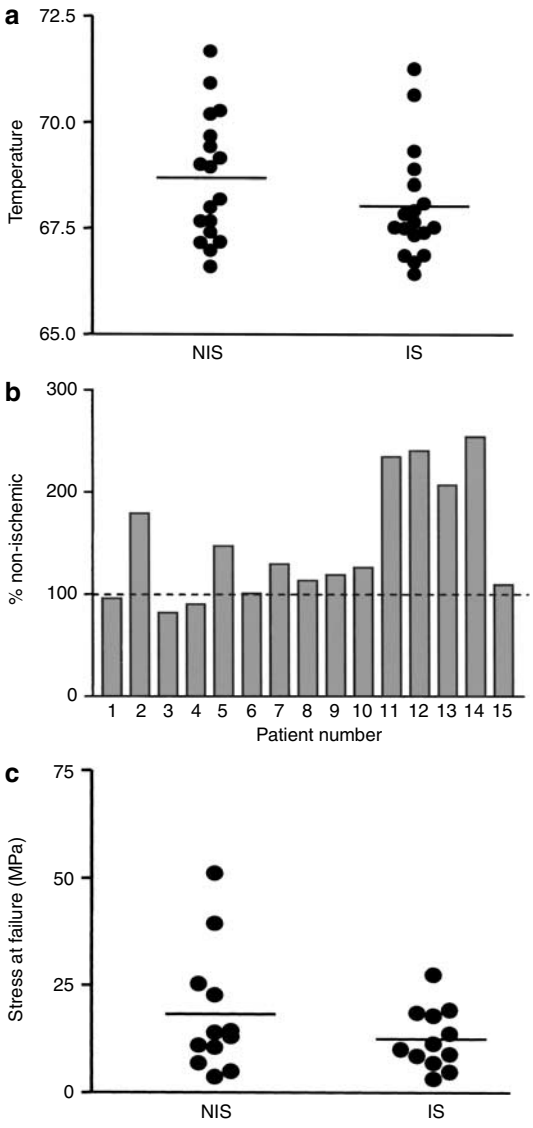

Figure 8. Properties of IS. (**a**) The thermal stability (temperature of denaturation; T_{max}) of the collagen molecule, measured by differential scanning calorimetry, was significantly lower in IS compared with NI controls ($P=0.02$, Wilcoxon's signed rank test). Results expressed as a percent of NI. (**b**) Susceptibility of collagen to pepsin digestion, measured by hydroxyproline release. IS is significantly more disposed to enzymic degradation than NIS ($P=0.01$, Wilcoxon's signed rank test). (**c**) Mechanical strength (stress at ultimate failure; Mpa) of IS was significantly lower than NI control skin ($P<0.05$, Wilcoxon's signed rank test).

three-dimensional collagen gels (Vinals and Pouyssegur, 2001), to induce production of VEGF (Berse *et al.*, 1999). VEGF promotes endothelial cell growth and survival (Carmeliet, 2000). Increased levels of VEGF protein in IS indicate activation of the oxygen-sensing transcription factor, hypoxia inducible factor-1α, which binds to a response element in the VEGF gene promoter. Detmar *et al.* (1997) showed that VEGF mRNA expression was dramatically upregulated in keratinocytes and fibroblasts from human skin explants in response to hypoxia and Berse *et al.* (1999) showed that such conditions doubled the rate of VEGF secretion stimulated by TGF-β1. We have demonstrated a significant increase in VEGF in uninjured but chronically ischemic skin, probably mediated via hypoxia inducible factor-1α and an upregulation of TGF-β1.

VEGF regulates endothelial cell proliferation, survival, and morphogenesis via VEGFRI and RII (Carmeliet, 2000). Elevated levels of VEGF in IS probably led to the raised endothelial VEGFRII expression and greater area of $CD105^+$ endothelium, a marker for angiogenesis used previously (Vermeulen *et al.*, 1996). We have demonstrated that CD105 is clearly expressed by endothelium in normal skin blood vessels and expression increased in chronic ischemia. Detmar *et al.* (1997) showed that both VEGFRI and RII mRNA were expressed at very low levels in normal skin and that hypoxia upregulated mRNA for both receptors in explant culture. VEGFRI, which is upregulated by hypoxia via hypoxia inducible factor-1α (Gerber *et al.*, 1997), acts as a negative regulator of VEGF signaling, allowing controlled vascular morphogenesis (Kearney *et al.*, 2004). It was expressed at relatively low levels in both ischemic and non-ischemic skin; however, there were patches of intense expression in endothelium and surrounding cells in the papillary dermis in some ischemic samples, possibly indicating areas of lowest oxygen tension. Blood vessels formed in tumors, which are considered hypoxic, and may lack basement membranes or pericytes, resulting in ineffective function (Sivridis *et al.*, 2003). Therefore, areas where $CD105^+$ endothelium occurred without concordant expression of type IV collagen provide some evidence for defective angiogenesis in chronically ischemic skin.

We have previously shown that increased collagen synthesis in IS does not result in increased net collagen deposition (Dalton *et al.*, 2005). Evidence here suggests that this may be a result of instability in the collagen molecule (Dalton *et al.*, 2003). Proline hydroxylation in collagen is essential for its molecular stability as hydroxyproline forms H-bonded water bridges through the hydroxyl group and the peptide chain (Kivirikko and Pihlajaniemi, 1998). In scurvy, for example, unstable under-hydroxylated type IV collagen deposition results in impaired angiogenesis (Mahmoodian and Peterkofsky, 1999), owing to reduced prolyl-4-hydroxylase activity resulting from lack of ascorbate, an essential cofactor for prolyl-4-hydroxylase. Impaired collagen hydroxylation may also occur in hypoxic conditions (Alper *et al.*, 1982), as oxygen is also an essential coreagent. This would also result in unstable collagen, including types I, III, and IV, leading to dysfunctional angiogenesis, increased susceptibility to denaturation and proteolytic degradation, and reduced mechanical strength.

There was direct evidence that the inappropriate matrix turnover combined with hypoxia in chronically ischemic, uninjured skin led to a destabilized collagen triple helix and weakened skin. Collagen stability was assessed using differential scanning calorimetry. T_{max} represents the thermal stability of the triple helix, which is strongly influenced by the presence of hydroxyproline residues, with one in seven proline molecules hydroxylated in normal collagen. The significant reduction in T_{max} in IS demonstrates reduced molecular stability of the collagen and implies reduced

hydroxyproline content, which may be expected in conditions of oxygen deficiency and inhibition of prolyl-4-hydroxylase. Resistance to proteolytic attack is a characteristic of stable triple helical collagen, and reduced stability of the collagen molecule may also result in increased susceptibility to proteolytic degradation, as demonstrated by increased dissolution of collagen by pepsin in the ischemic samples. Increased susceptibility to digestion by nonspecific proteases is also important in the pathology of ulceration, reducing strength and increasing the predisposition to dermal breakdown. Despite the technical difficulties in determining mechanical strength of skin, we were able to demonstrate that IS is indeed weaker than matched paired NIS controls.

In this study, we have demonstrated increases in lactate, TGF-β levels and signaling, VEGF, and angiogenesis, all normally associated with tissue repair processes, yet here manifest in uninjured, non-inflamed, but chronically ischemic skin. This results in increased collagen synthesis and remodeling (Dalton *et al.*, 2005). Simultaneous with this, the newly deposited collagen is both unstable and more susceptible to enzyme digestion (Dalton *et al.*, 2003). As a consequence of these two processes, the skin is weakened and more susceptible to breakdown, and angiogenesis is impaired, possibly exacerbating the ischemia at a local level. We propose a novel mechanistic model for dermal breakdown in ulceration. Tissue exposure to chronic oxygen deprivation in ischemia leads to secretion of inappropriate levels of TGF-β and VEGF, resulting in increased collagen synthesis and raised levels of degradative MMPs. The collagen produced in a low-oxygen environment is unstable as a result of oxygen deficiency in molecular and fibrillar stabilization processes. This unstable collagen is weaker and has increased susceptibility to proteolytic attack, in an environment with increased expression of degradative MMPs. These factors lead to a weakened dermis and a predisposition to chronic ulceration, which may occur after relatively minor trauma to the skin.

This study provides insights into mechanisms in skin ulceration, and potential clinical targets, such as reducing collagen turnover or optimizing tissue oxygen utilization by, for instance, upregulating prolyl-4-hydroxylase. It is recognized that the de-stabilization of collagen identified here may be a factor in other degenerative diseases where rapid or elevated matrix turnover occurs alongside hypoxia. This may be important in diseases such as intervertebral disc degeneration, osteoarthritis, and tendonitis, as well as other ischemic disorders.

MATERIALS AND METHODS

Unless otherwise stated, reagents were obtained from Sigma (Poole, UK). Procedures involving human subjects were approved by all appropriate local Ethical Review Panels, and comply with the World Medical Association Declaration of Helsinki on Ethical Principles for Medical Research.

Sample collection and preparation

Following written informed consent, 8-mm skin biopsies were taken at operation from the lower limbs of 21 patients (10 female, 11 male, mean age 72; range, 62–84) undergoing below-knee amputation for peripheral vascular disease, from both proximal (NIS) and distal (IS) sites as described previously (Dalton *et al.*, 2005). Patients had documented peripheral vascular disease for at least a year, with ankle brachial pressure ratios of less than 0.4 indicating severe ischemia. Control skin taken at TKR ($n=7$, mean age 71; range, 57–81) and VV ($n=8$, mean age 55; range 34–68) surgery was used as proximal- and distal site-matched controls, respectively. Assessment of patients, determination of ischemia, and sample preparation were as described previously (Dalton *et al.*, 2005). Tissue was pulverized, freeze dried, and extracted for 24 hours in 20 μl of extract buffer (20 mM triethanolamine and 0.1% Brij) per mg dry weight, the mixture centrifuged, and supernatant separated from the insoluble matrix pellet. Fat extraction was performed on the pellet using 2:1 chloroform/methanol, in order to establish the true dry mass of the skin, which was used in all compositional calculations. Samples were stored at -80°C until required.

Tissue lactate

Samples were examined in matched pairs. Freeze dried tissue was re-suspended at 2 mg/μl in phosphate-buffered saline (PBS). Samples were mixed at 4°C, centrifuged for 5 minutes at 13,000 $\times$ *g*, and supernatants were tested for lactate using colorimetric enzymatic determination (Sigma) on a 96-well assay plate. Absorbance was read at 540 nm. Concentrations of lactate were calculated against a standard curve using Labsystems Genesis software (ThermoLife Science Int, Basingstoke, UK).

TGF-β1

Total TGF-β1 levels were assessed by ELISA in acid-activated sample extract (50 μl) in triplicate as described previously (Whiting *et al.*, 2001).

Immunohistology

Matched pairs of frozen sections were processed and analyzed for TGF-βRI, TGF-βRII, TGF-βRIII, CD105, phosphorylated-smad2/3, smad7, CD45, VEGFRI, VEGFRII, and type IV collagen using peroxidase conjugates or multiple immunofluorescence. All antibodies are listed in Table 1.

Eight-micron frozen sections from matched pairs were cut onto the same slide, air-dried, fixed in acetone at 4°C for 10 minutes and then rehydrated in PBS for 10 minutes. Nonspecific binding was blocked with sera +/− non-fat milk powder in PBS for 1 hour at 20°C (Table 1), followed by an avidin/biotin block (Vector Laboratories, Peterborough, UK). Owing to nonspecific binding of rabbit IgG a stringent blocking procedure was used as follows. Following 1% normal rabbit serum block (Table 1), sections were incubated with 1:25 donkey anti-rabbit Fab (Stratech, West Grove, PA). Primary antibodies, or equivalent immunoglobulin controls, were added to sections at concentrations listed in Table 1 and incubated at 4°C overnight. Sections were washed in PBS and then biotinylated secondary antibodies (Stratech) were applied for 1 hour at 20°C. Staining was developed using either (1) peroxidase-conjugated Streptavidin biotin complexes (Vector) with diamino benzidene as substrate followed by a light counter-stain with Mayers hematoxylin, dehydration and mounting or (2) streptavidin-dichlorotriazinyl amino fluoriscein (DTAF)

Table 1. Primary and secondary antibodies

Antibody	Code/clone	Host	Serum block	Concentration (μg/ml)	Source
Target					
TGF-β RI	sc-398	Rabbit	NDS 10%, NRS 1%	4	SC
TGF-β RII	sc-400	Rabbit	NDS 10%, NRS 1%	1	SC
TGF-β RIII	sc-6199	Rabbit	NDS 10%, NRS 1%	1	SC
Smad7	sc9183	Goat	NDS 10%	4	SC
P-Smad2/3	3101	Rabbit	NDS 10%		
			NRS 1%	2	CS
CD45	MCAP87	Mouse	NRS 10%	5	SE
Collagen IV	AD4	Mouse	NRS 10%	1	GP
VEGF RI	MAB321	Mouse	NRS 10%		
			MP 5%	10	R&D
VEGF RII	AF357	Goat	NDS 10%	0.5	R&D
CD105	AF1097	Goat	NDS 10%	0.5	R&D
Secondary					
Rabbit-biotin	711-065-152	Donkey		1:500	ST
Goat-biotin	705-065-147	Donkey		1:500	ST
Mouse-biotin	E0354	Rabbit		1:200	D
Goat-FITC	705-095-147	Donkey		1:50	ST
SA:	016-010-084			1:250	ST
SA-Texas red	SA-5006			1:100	V

CS, Cell Signaling Technology Inc. (Danvers, MA); D, DAKO (Glostrup, Denmark); FITC, fluorescein isothiocyanate; NDS, normal donkey serum; NRS, normal rabbit serum; MP, non-fat milk powder; R&D (Abingdon, UK); SA, streptavidin; SC, Santa Cruz Biotechnology (Santa Cruz, CA); SE, Serotec (Kidlington, UK); ST, Stratech (Cambridge, UK); TGF, transforming growth factor; V, Vector (Peterborough, UK); VEGF, vascular endothelial growth factor. GP is a kind gift from Dr Gordon Paul, Institute of Leather, Nottingham, UK.

(Table 1). For double labeling, primary antibodies were applied together overnight, followed by biotinylated anti-mouse and finally donkey anti-goat-FITC plus streptavidin, Texas Red. Images were viewed using a Leica DMRB microscope (Leica UK, Milton Keynes, UK) and grabbed using a Colour Coolview charge coupled device camera (Photonic Sciences, Robertsbridge, E Sussex, UK) and Image-Pro Plus software (Media Cybernetics, Baltimore, MD).

Peroxidase-stained sections were analyzed for the area of dermis expressing CD105 using images grabbed with the ×10 objective. RGB profiles for positive expression was determined using levels at least twice background intensity in each channel. Six fields were grabbed per sample and the area of analysis defined to exclude epidermis. Results are expressed as (μm^2) CD105+ endothelium/μm^2 dermis. Samples were coded, processed in matched pairs, and analyzed blind.

Collagen synthesis

Type I collagen C propeptide (PICP) was quantitated by ELISA (Prolagen C™, Quidel, Oxon, UK). Tissue extracts were diluted 1:12 in assay buffer and absorbance read at 405 nm. PICP concentrations were calculated against a standard curve using Labsystems Genesis software (Tarlton *et al.*, 1999).

VEGF

VEGF was measured by ELISA (R&D, Oxford, UK). Tissue extracts were diluted 1:3 in PBS and absorbance read at 450 nm. Concentrations of sample VEGF were calculated against a standard curve using Labsystems Genesis software.

Molecular stability

The molecular stability of the collagen triple helix determines the energy required to bring about denaturation. The heat capacity is a measure of the energy of denaturation, and may be quantified by differential scanning calorimetry (Miles *et al.*, 1995). Unprocessed tissue (5 mg) was thawed at room temperature, re-hydrated for 1 hour in PBS to ensure comparable hydration and pH, and sealed into a pre-weighed aluminum pan (Perkin Elmer, Beaconsfield, UK). A baseline reading was obtained by loading two empty pans onto a Perkin Elmer differential scanning calorimetry-2 calorimeter before loading samples. Samples were heated from 10 to 110°C at a rate of 10°C per minute using nitrogen as the flushing gas and a thermogram was generated. The pans were then punctured to release the seal, freeze dried overnight, reweighed to determine the sample dry weight and then hydrolyzed in 5 ml 6 M HCL. Hydrolysates were reconstituted in water and the total collagen content calculated using hydroyproline analysis as described previously (Dalton *et al.*, 2005). From the thermogram, T_{max} is recorded as the temperature at maximum heat capacity.

Susceptibility to enzymic degradation

Resistance to proteolytic attack is a characteristic of triple helical collagen. Increased susceptibility to nonspecific proteolysis is important in the ulcer pathology, as well as a measure of molecular

stability (Danielsen, 1990). Approximately 5 mg of pulverized tissue was incubated with 250 μl 0.4 mg/ml pepsin in 0.5 M acetic acid for 60 hours at 30°C. The digest was separated from the residual pellet by centrifugation at 13,000 × *g*, and both the supernatant and pellet were analyzed for collagen content as described above. Susceptibility to pepsin digestion was expressed as the percentage of the total hydroxyproline released into solution.

Mechanical strength

Longitudinal skin samples (25 × 10 mm) were taken without tension and excess fat was excised. The skin was dried between layers of filter paper in order to remove excess tissue fluid, and was fashioned into a dumbbell shape using a punch biopsy tool, giving a standard central width of 2.5 mm.

The cornified layer was then gently removed with emery paper over the sample ends in order to prevent sloughing stratum cornea causing slippage in the clamps. Emery paper was cut into 15 × 30 mm rectangles, scored and folded to give double-sided squares with the abrasive surface facing inward. Loctite 406 cyanoacrylate adhesive (Loctite, Welwyn Garden City, Herts, UK) was added to one of these surfaces and the distal 10 mm of our skin sample placed epithelial surface down onto this. A longitudinal incision was then made centrally through the end 5 mm of the adhered sample on the exposed side in order to divide any hypodermis present and the sample was spatulated. Adhesive was applied to the upper surface and the emery paper folded over and held for 1 minute. The process was then repeated for the other end of the sample, leaving a 5 mm hourglass-shaped skin section between squares of emery paper. Specimens were loaded onto an Instron 6033 materials testing apparatus (Instron, High Wycombe, UK) using 100 N static load cell and gripped with pneumatic clamps set to 120 N/m^2. Slack taken up by loading the skin to 0.5 N. The thickness and width of the sample were then measured using vernier calipers.

Skin samples were loaded to failure at a strain rate of 1 cm/min and data recorded using a PC equipped with series IX data acquisition and analysis software (Instron). A load-deformation curve was constructed from which the maximum load (F_{max}) at failure was obtained. Breaking stress was then calculated as F_{max} (N)/original cross-sectional area (mm^2), and expressed as MPa.

Statistical analyses

All data are expressed as the mean ± SEM. Two-tailed Wilcoxon-matched pairs signed ranks tests were performed on paired data, with unpaired *t*-tests on controls, using Instat© software. Probabilities are given as *P*-values, with $P<0.05$ regarded as significant. Normality of the data was assessed using Instat software and corrected where necessary with a Welch correction.

CONFLICT OF INTEREST

The authors state no conflict of interest.

ACKNOWLEDGMENTS

This work was funded by Action Medical Research, with additional support from The Southmead Research Fund and The European Society for Vascular and Endovascular Surgery.

REFERENCES

Akikusa JD, Garrick D, Nash MC (2003) Scurvy: forgotten but not gone. *J Paediatr Child Health* 39:75–7

Alper R, Kerr JS, Kefalides NA, Fisher AB (1982) Relation between reduced alveolar PO2 and collagen biosynthesis in the perfused rat lung. *J Lab Clin Med* 99:442–50

Berse B, Hunt JA, Diegel RJ, Morganelli P, Yeo K, Brown F *et al.* (1999) Hypoxia augments cytokine (transforming growth factor-beta (TGF-beta) and IL-1)-induced vascular endothelial growth factor secretion by human synovial fibroblasts. *Clin Exp Immunol* 115:176–82

Bettinger DA, Yager DR, Diegelmann RF, Cohen IK (1996) The effect of TGF-beta on keloid fibroblast proliferation and collagen synthesis. *Plast Reconstr Surg* 98:827–33

Carmeliet P (2000) Mechanisms of angiogenesis and arteriogenesis. *Nat Med* 6:389–95

Constant JS, Feng JJ, Zabel DD, Yuan H, Suh DY, Scheuenstuhl H *et al.* (2000) Lactate elicits vascular endothelial growth factor from macrophages: a possible alternative to hypoxia. *Wound Repair Regen* 8: 353–60

Cornwall JV, Dore CJ, Lewis JD (1986) Leg ulcers: epidemiology and aetiology. *Br J Surg* 73:693–6

Dalton SJ, Mitchell DC, Tarlton JF (2003) Altered crosslinking and thermal stability of collagen in chronically ischaemic skin. In: Proceedings of the Thirteenth European Tissue Repair Society. Amsterdam: The Netherlands (Abstr.)

Dalton SJ, Mitchell DC, Whiting CV, Tarlton JF (2005) Abnormal extracellular matrix metabolism in chronically ischemic skin: A mechanism for dermal failure in leg ulcers. *J Invest Dermatol* 125:373–9

Danielsen CC (1990) Age-related thermal stability and susceptibility to proteolysis of rat bone collagen. *Biochem J* 272:697–701

Detmar M, Brown LF, Berse B, Jackman RW, Elicker BM, Dvorak HF *et al.* (1997) Hypoxia regulates the expression of vascular permeability factor/vascular endothelial growth factor (VPF/VEGF) and its receptors in human skin. *J Invest Dermatol* 108:263–8

Duff SE, Li C, Garland JM, Kumar S (2003) CD105 is important for angiogenesis: evidence and potential applications. *FASEB J* 17: 984–92

Falanga V, Qian SW, Danielpour D, Katz MH, Roberts AB, Sporn MB (1991) Hypoxia upregulates the synthesis of TGF-beta 1 by human dermal fibroblasts. *J Invest Dermatol* 97:634–7

Falanga V, Zhou L, Yufit T (2002) Low oxygen tension stimulates collagen synthesis and COL1A1 transcription through the action of TGF-beta1. *J Cell Physiol* 191:42–50

Geiser AG, Burmester JK, Webbink R, Roberts AB, Sporn MB (1992) Inhibition of growth by transforming growth factor-beta following fusion of two nonresponsive human carcinoma cell lines. Implication of the type II receptor in growth inhibitory responses. *J Biol Chem* 267:2588–93

Gerber HP, Condorelli F, Park J, Ferrara N (1997) Differential transcriptional regulation of the two vascular endothelial growth factor receptor genes. Flt-1, but not Flk-1/KDR, is up-regulated by hypoxia. *J Biol Chem* 272:23659–67

Harrington C, Zagari MJ, Corea J, Klitenic J (2000) A cost analysis of diabetic lower-extremity ulcers. *Diabetes Care* 23:1333–8

Hunt TK, Conolly WB, Aronson SB, Goldstein P (1978) Anaerobic metabolism and wound healing: an hypothesis for the initiation and cessation of collagen synthesis in wounds. *Am J Surg* 135:328–32

Johnson JA, Fusaro RM (1972) The role of the skin in carbohydrate metabolism. *Adv Metab Disord* 60:1–55

Kearney JB, Kappas NC, Ellerstrom C, DiPaola FW, Bautch VL (2004) The VEGF receptor flt-1 (VEGFR-1) is a positive modulator of vascular sprout formation and branching morphogenesis. *Blood* 103:4527–35

Kivirikko KI, Pihlajaniemi T (1998) Collagen hydroxylases and the protein disulfide isomerase subunit of prolyl 4-hydroxylases. *Adv Enzymol Relat Areas Mol Biol* 72:325–98

Klein MB, Pham H, Yalamanchi N, Chang J (2001) Flexor tendon wound healing *in vitro*: the effect of lactate on tendon cell proliferation and collagen production. *J Hand Surg (America)* 26:847–54

London NJ, Donnelly R (2000) ABC of arterial and venous disease. Ulcerated lower limb. *Br Med J* 320:1589–91

Lopez-Casillas F, Wrana JL, Massague J (1993) Betaglycan presents ligand to the TGF beta signaling receptor. *Cell* 73:1435–44

Mahmoodian F, Peterkofsky B (1999) Vitamin C deficiency in guinea pigs differentially affects the expression of type IV collagen, laminin, and elastin in blood vessels. *J Nutr* 129:83–91

Miles CA, Burjanadze TV, Bailey AJ (1995) The kinetics of the thermal denaturation of collagen in unrestrained rat tail tendon determined by differential scanning calorimetry. *J Mol Biol* 245:437–46

Mogford JE, Tawil N, Chen A, Gies D, Xia Y, Mustoe TA (2002) Effect of age and hypoxia on TGFbeta1 receptor expression and signal transduction in human dermal fibroblasts: impact on cell migration. *J Cell Physiol* 190:259–65

Mortazavi-Haghighat R, Taghipour-Khiabani K, David S, Kerrigan CL, Philip A (2002) Rapid and dynamic regulation of TGF-beta receptors on blood vessels and fibroblasts during ischemia-reperfusion injury. *Am J Physiol Cell Physiol* 282:C1161–9

Nanney L (2005) Looking beneath the surface–setting the stage for skin ulceration. *J Invest Dermatol* 125:vii–i

Petersen LJ (1999) Interstitial lactate levels in human skin at rest and during an oral glucose load: a microdialysis study. *Clin Physiol* 19:246–50

Roberts DM, Kearney JB, Johnson JH, Rosenberg MP, Kumar R, Bautch VL (2004) The vascular endothelial growth factor (VEGF) receptor Flt-1 (VEGFR-1) modulates Flk-1 (VEGFR-2) signaling during blood vessel formation. *Am J Pathol* 164:1531–5

Salo T, Lyons JG, Rahemtulla F, Birkedal-Hansen H, Larjava H (1991) Transforming growth factor-beta 1 up-regulates type IV collagenase expression in cultured human keratinocytes. *J Biol Chem* 266:11436–41

Sanchez-Elsner T, Botella LM, Velasco B, Corbi A, Attisano L, Bernabeu C (2001) Synergistic cooperation between hypoxia and transforming growth factor-beta pathways on human vascular endothelial growth factor gene expression. *J Biol Chem* 276:38527–35

Sanchez-Elsner T, Botella LM, Velasco B, Langa C, Bernabeu C (2002) Endoglin expression is regulated by transcriptional cooperation between the hypoxia and transforming growth factor-beta pathways. *J Biol Chem* 277:43799–808

Shen BQ, Lee DY, Gerber HP, Keyt BA, Ferrara N, Zioncheck TF (1998) Homologous up-regulation of KDR/Flk-1 receptor expression by vascular endothelial growth factor *in vitro*. *J Biol Chem* 273:29979–85

Sivridis E, Giatromanolaki A, Koukourakis MI (2003) The vascular network of tumours–what is it not for? *J Pathol* 201:173–80

Stampfer MR, Yaswen P, Alhadeff M, Hosoda J (1993) TGF beta induction of extracellular matrix associated proteins in normal and transformed human mammary epithelial cells in culture is independent of growth effects. *J Cell Physiol* 155:210–21

Strutz F, Zeisberg M, Renziehausen A, Raschke B, Becker V, Van Kooten C *et al*. (2001) TGF-beta 1 induces proliferation in human renal fibroblasts via induction of basic fibroblast growth factor (FGF-2). *Kidney Int* 59:579–92

Tarlton JF, Bailey AJ, Crawford E, Jones D, Moore K, Harding KD (1999) Prognostic value of markers of collagen remodeling in venous ulcers. *Wound Repair Regen* 7:347–55

Vermeulen PB, Gasparini G, Fox SB, Toi M, Martin L, McCulloch P *et al*. (1996) Quantification of angiogenesis in solid human tumours: an international consensus on the methodology and criteria of evaluation. *Eur J Cancer* 32A:2474–84

Vinals F, Pouyssegur J (2001) Transforming growth factor beta1 (TGF-beta1) promotes endothelial cell survival during *in vitro* angiogenesis via an autocrine mechanism implicating TGF-alpha signaling. *Mol Cell Biol* 21:7218–30

Whiting CV, Williams AM, Claesson MH, Bregenholt S, Reimann J, Bland PW (2001) Transforming growth factor-beta messenger RNA and protein in murine colitis. *J Histochem Cytochem* 49:727–38

Wong SH, Hamel L, Chevalier S, Philip A (2000) Endoglin expression on human microvascular endothelial cells association with betaglycan and formation of higher order complexes with TGF-beta signalling receptors. *Eur J Biochem* 267:5550–60

Wrana JL, Attisano L, Wieser R, Ventura F, Massague J (1994) Mechanism of activation of the TGF-beta receptor. *Nature* 370:341–7

Yalamanchi N, Klein MB, Pham HM, Longaker MT, Chang J (2004) Flexor tendon wound healing *in vitro*: lactate up-regulation of TGF-beta expression and functional activity. *Plast Reconstr Surg* 113: 625–32